

A Theoretical Investigation of the Physical Reason for the Very Different Luminescence Properties of the Two Isomers Adenine and 2-Aminopurine

Anders Broo

Department of Physical Chemistry, Chalmers University of Technology, 412 96 Göteborg, Sweden

Received: April 21, 1997; In Final Form: October 6, 1997

The geometry of the ground state and the first singlet excited state of adenine and 2-aminopurine was calculated with three different quantum chemical methods: AM1, CIS/6-31G, and CASSCF/6-31G. Three possible deactivation mechanisms or reactions of excited molecule were considered: the pseudo Jahn–Teller distortion, excited-state tautomerism, and formation of so-called twisted intramolecular charge transfer (TICT) states. Different mechanisms for the nonradiative decay are operative for the two isomers. The geometrically relaxed excited state of adenine has $n \rightarrow \pi^*$ character, while it has $\pi \rightarrow \pi^*$ character for 2-aminopurine. The state crossing that occurs during the excited-state relaxation of adenine opens up an effective nonradiative deactivation channel not present for 2-aminopurine. Tautomerism in the excited state might explain the difference in luminescence quantum yield upon DNA binding for 2-aminopurine. The excited state of the *7H* tautomer of adenine undergoes a large geometry change during the relaxation, and the final geometry of the $n \rightarrow \pi^*$ state resembles a TICT state, but with only little charge transfer.

Introduction

The quantum yield for fluorescence is very low for all the DNA bases.¹ It is most likely that the evolution has chosen material that has a minimal luminescence and short excited-state lifetime to diminish photoreactions in the living cells. In this context it is very interesting to note that the two isomers, adenine (Ade) and 2-aminopurine (2AMP), have such different quantum yields. While the quantum yield for fluorescence is around 0.5 for 2AMP, it only about 0.0003 for Ade.^{1,2} The absorption spectra in the low-energy region are rather different. Ade has an absorption maximum at about 37 000 cm^{-1} , while the low-energy band maximum for 2AMP is found at about 32 000 cm^{-1} . Furthermore, 2AMP base pairs with thymine in a similar way as does adenine; thus, 2AMP preserves the B-form DNA. These properties have been used to study structure and dynamics of DNA fragments by replacing Ade with the fluorescent isomer 2AMP.^{3,4}

The emission quantum yield of 2AMP has been found to be rather sensitive to buffer concentration⁵ and solvent polarity.^{3,6} Furthermore, the quantum yield decreases 3–10-fold upon DNA binding. In a recent work, Santhosh and Mishra⁷ found from excited-state lifetime measurements that the fluorescence decay had two components: one component had a lifetime of 2.1 ns, and the second lifetime was determined to be 24.6 ns. They concluded that two fluorescent species, the *9H* tautomer and the *7H* tautomer, were present in the experiment. Evidence for reabsorption of the very strong emission for 2AMP was also reported.⁷

In 1966, Longworth et al.⁸ investigated the luminescence properties of all the DNA bases. It was hinted that the major part of the emission of Ade arises from the *7H* tautomer. Later, Eastman⁹ determined the relative concentration of the *7H* tautomer to be 6% by comparing the emission spectra of 7-methyl- and 9-methyladenine with the emission spectra of

adenine. Wilson and Callis¹⁰ confirmed that indeed the major part of the fluorescence is attributed to the minor tautomer *7H*-adenine.

The objective for this work is to investigate the physical background for the very different emission properties of the two isomers, adenine (6-aminopurine) and 2-aminopurine. Several possible deactivation mechanisms might be operative. Lim¹¹ outlined a model for quenching of the luminescence of nitrogen heterocyclic and aromatic carbonyl components where vibronic coupling between nearby $n \rightarrow \pi^*$ and $\pi \rightarrow \pi^*$ states causes the quenching. This so-called proximity effect or pseudo Jahn–Teller distortion¹² accounts well for e.g. the observed solvent effects on the luminescence of 8-methoxypsoralen.¹¹ The vibrational mode that couples the $n \rightarrow \pi^*$ state with the $\pi \rightarrow \pi^*$ state is an out-of-plane vibration. If the vibrational coupling is large, the Franck–Condon factor associated with the radiationless transition is large, leading to a rapid conversion to the ground-state hypersurface. Photoinduced reactions such as tautomerism in the excited state possibly facilitated by a protic solvent that acts as proton acceptor and donor for the transferred proton, or large conformation changes such as twisted intramolecular charge transfer (so-called TICT states) might account for the differences in photophysics of the two isomers. Recently, Albinsson reported formation of a TICT state in *N*⁶,*N*⁶-dimethyladenosine, accompanied by a dual fluorescence.¹³ Quantum chemical calculations will be used to investigate the geometry of both the ground and the first excited state and the spectroscopy of the two molecules.

Computational Details

The ground-state and first singlet excited-state geometries have been fully optimized utilizing three methods. The ground-state geometries were fully optimized, and the stationary points were verified with a vibration spectrum analysis in a traditional way. The character of the stationary points on the first excited-

state hypersurface was never analyzed. The least computer resource demanding method used in this study of the excited-state geometries was the semiempirical AM1 method.¹⁴ The AM1 calculations were performed with the mopac 6.0 program.¹⁵ The AM1 ground-state geometries were calculated with the normal Hartree–Fock approximation. The AM1 excited-state geometries were calculated using a small configuration interaction (CI) where the active space consisted of two occupied π molecular orbitals (MO's) and two unoccupied π MO's, giving a CI calculation with four electrons in four orbitals. The abbreviation AM1-CI(4/4) will be used throughout in this paper. It has previously been shown that the first two $\pi \rightarrow \pi^*$ excited state of Ade is dominated by two singly excited configurations within this small CI space.^{1,16} Thus, the major contribution to the first excited state is expected to be included in the description.

Two ab initio methods were employed in this study of the excited-state geometries of Ade and 2AMP. Both the complete active space self-consistent-field (CASSCF) and the ab initio configuration interaction where only single excited configurations are included (CIS) are much more demanding on computer resources than is the AM1 method. The CASSCF calculations were performed with the GAMESS program,¹⁷ and the CIS calculations were done with the Gaussian94 program.¹⁸ The standard split-valence basis set 6-31G¹⁹ was used in both types of ab initio calculations of the ground- and excited-state geometries. This rather small basis set was selected to allow a comparison at an equal basis of the geometries obtained with the different methods. The CIS/6-31G geometry of 2AMP was then reoptimized with the 6-31G basis set augmented with a set of d-type polarization functions on the non-hydrogen atoms. Only small geometry changes and spectroscopic changes were obtained using the larger basis set. Thus, all the reported CIS geometries and all CIS spectra, except the absorption spectrum, are with the 6-31G basis set. As comparison, INDO/S-CI spectra are also reported. The ZINDO program²⁰ was used, and the CI space included all single excitations with $\pi \rightarrow \pi^*$ and $n \rightarrow \pi^*$ character. Typically around 100 singly excited configurations were included in the CI. The standard parametrization was used, and the Mataga–Nishimoto approximation was used to calculate the two-electron repulsion integrals.

Results and Discussion

Ground- and Excited-State Geometries. It is nowadays well-known that to accurately reproduce the observed geometries of the DNA bases correlation corrected methods have to be used.^{21–24} However, at present it is not feasible to optimize the geometry of excited states of such large molecules with a proper account for the dynamical electron correlation. Thus, simpler methods must be used. First, the reliability of the used methods is evaluated by comparing the geometries of the first excited state and of the ground state obtained with the three methods. The most important geometrical parameters of the ground state of Ade and 2AMP are collected in Figure 1. The difference in predicted bond lengths is small for most of the bonds. However, some bond lengths are calculated to be very different with the three methods. Without polarization functions both the HF and the CASSCF methods predict planar geometries, while inclusion of polarizations functions introduces some nonplanarity in the amino group. For Ade, the unsigned average errors of the predicted bond lengths are 0.028 Å (AM1), 0.016 Å (HF/6-31G*), and 0.013 Å (CASSCF/6-31G) compared with the neutron diffraction geometry of 9-methyladenine. The

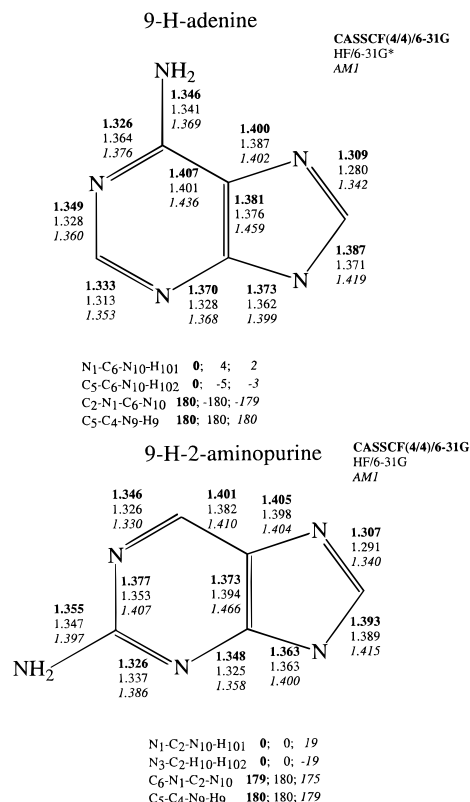


Figure 1. Comparison of a selection of geometrical parameters of 9H-adenine and 9H-2-aminopurine, as predicted with the CASSCF, HF, and AM1 methods.

corresponding errors for 2AMP are 0.035 Å (AM1), 0.012 Å (HF/6-31G), and 0.018 Å (CASSCF/6-31G). The ground-state geometries are reasonably well reproduced with all methods. Adding polarization functions at the HF level of theory has only a modest influence on the final geometry. A sufficient account for the electron correlation, at for instance the MP2 level of theory, has a larger effect on the predicted geometries.^{16,24} Of course, polarization functions are necessary in such calculations.

There is no experimental method to directly determine excited-state geometries of molecules of this size. Under the assumption that electron correlation is of equal importance for the geometry of the excited states as for the ground state, the AM1-CI(4/4), CIS/6-31G, and CASSCF(4/4)/6-31G methods are used to predict the geometry of the first excited state of Ade and 2AMP. The geometry of the first singlet excited state of Ade as predicted with the three different methods is shown in Figure 2. All three methods predict a rather puckered geometry. The AM1-CI(4/4) and CASSCF(4/4) methods predict that the first singlet excited state has $\pi \rightarrow \pi^*$ character, while the CIS method results in a state having $n \rightarrow \pi^*$ character. The $n \rightarrow \pi^*$ state was not included in the restricted CI space in either of the AM1-CI(4/4) and CASSCF(4/4) calculations. The CIS geometry optimization had serious convergence problems since the character of the first excited state changed during the optimization. The character of the lowest energy excited state ($n \rightarrow \pi^*$) was confirmed by starting the geometry optimization from several different starting geometries. The $\pi \rightarrow \pi^*$ state, that is the first excited state of the vertical transition spectrum, has an almost stationary point on the potential energy surface. The geometry of that state differs from the $n \rightarrow \pi^*$ state in the N1–C2–N3 part of the molecule. The $\pi \rightarrow \pi^*$ state has an N1–C2 bond length of 1.334 Å, while in the $n \rightarrow \pi^*$ state the N1–C2 bond is 1.388 Å. A marked out-of-plane displacement of the C2–

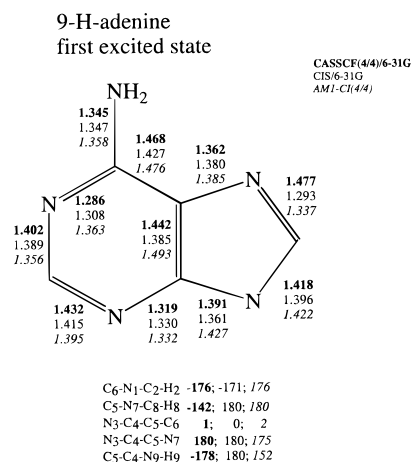


Figure 2. Selection of geometrical parameters for the first singlet excited state of 9H-adenine as predicted with the CASSCF, CIS, and AM1 methods.

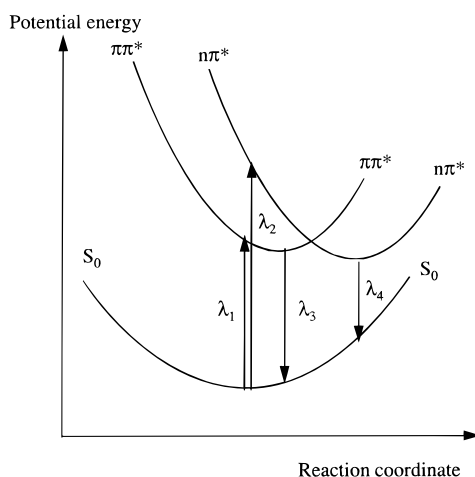


Figure 3. Schematic representation of the ground state and the two first excited states of 9H-Ade. λ_1 and λ_2 denote the absorption wavelengths and λ_3 and λ_4 denote the emission wavelengths when the emission starts from the $\pi \rightarrow \pi^*$ state and from the $n \rightarrow \pi^*$ state, respectively. In reality, the potential energy surfaces are multidimensional and the reaction coordinate is rather complicated.

H₂ group is found in the $n \rightarrow \pi^*$ state, while the $\pi \rightarrow \pi^*$ is almost planar. The largest out-of-plane displacement observed in the AM1-CI(4/4) geometry is for the hydrogen bonded to N₉. For the CASSCF(4/4) geometry the largest out-of plane displacement is found for the hydrogen bonded to C₈. A schematic representation of the three states as calculated by the CIS/6-31G method is displayed in Figure 3. At the crossing point (so-called avoided crossing) of the two excited-state curves the magnitude of the vibronic coupling could be extracted as the energy difference between the two states. At the avoided crossing the two states are completely mixed and have both $n \rightarrow \pi^*$ character and $\pi \rightarrow \pi^*$ character. This will be further discussed in the spectroscopy section.

The predicted geometries of the first singlet excited state of 2AMP are shown in Figure 4. All three methods predict the geometry-relaxed first excited state to have $\pi \rightarrow \pi^*$ character. Now, both the CIS and the CASSCF methods give rather planar geometries. The AM1 method gives a more puckered geometry with a large out-of-plane displacement of the hydrogen bonded to N₉. As a further test of the basis set dependence on the excited-state geometry, the geometry of the first singlet excited state of 2AMP was reoptimized at the CIS/6-31G* level of theory. Only minor changes of the geometry were observed.

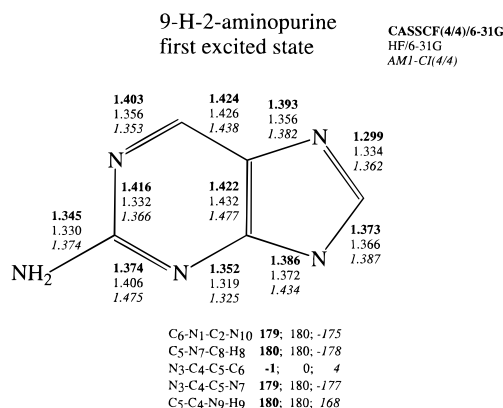


Figure 4. Selection of geometrical parameters for the first singlet excited state of 9H-2-aminopurine as predicted with the CASSCF, CIS, and AM1 methods.

All three methods give similar geometries of both the ground state and the first singlet excited state. From a methodological point of view the CIS method and the CASSCF(4/4) method are about equally demanding on computer resources. The CASSCF(4/4) method introduces some electron correlation both in the ground and in the excited states, but the necessary restriction in active space does not allow for inclusion of excitations of $\sigma \rightarrow \sigma^*$ type in the CI wave function. In a recent work Broo pointed out the importance of such $\sigma \rightarrow \sigma^*$ excitations for the description of the $\pi \rightarrow \pi^*$ transitions of benzene.²⁵ Benzene is a case where the size of the dynamical electron correlation is not the same for all the excited states, and the CIS/6-31G method fails seriously to predict the observed absorption spectrum. However, if some of the $\sigma \rightarrow \sigma^*$ transitions are excluded from the active space, the transition energies could be linearly scaled to agree with the observed transition energies.²⁵ Based on previous experience, the CIS/6-31G method is used for the further studies of the photophysics of the two isomers.

Ground- and Excited-State Tautomerism. It has been shown both theoretically²⁴ and experimentally⁹ that Ade exists in two tautomeric forms (9H-Ade and 7H-Ade) in water solution, with the 9H tautomer as the major component. Furthermore, it has been shown that the major part of the emission of Ade comes from the 7H tautomer. Santhosh and Mishra suggested that the two-component decay of the emission of 2AMP in ethanol was due to tautomerism. Broo and Holmén have investigated the tautomeric equilibrium in the ground state of both Ade and 2AMP.²⁴ At the HF/6-31G* level of theory the relative energy difference between the two tautomers, ΔE , was 38.7 kJ/mol. At the MP2/6-31G* level of theory an ΔE of 33.1 kJ/mol was obtained, and at the MP4(SDQ)/6-31G**/MP2/6-31G* level of theory ΔE was calculated to 34.3 kJ/mol. Thus, electron correlation had only small effects on the relative stability of the two tautomers. Solvent effects as accounted for by a self-consistent reaction field had a much larger impact on ΔE . The solution ΔE was brought down to between 6.7 and 10.2 kJ/mol, due to the different charge distribution in the two tautomers. The corresponding ΔE for 2AMP, calculated at the MP2/6-31G* level of theory, are 18.8 kJ/mol (vacuum) and 11.2 kJ/mol (water).

In this work, the relative energies of the first singlet excited state of the 9H-Ade and 7H-Ade and 9H-2AMP and 7H-2AMP are calculated at the CIS/6-31G level of theory. The geometries were optimized in a traditional way in the vacuum, and no difference in zero-point vibration energy is included in the reported ΔE values. The 9H tautomer is the most stable

TABLE 1: Adenine Vertical Transition Energies Predicted by the CIS/6-31G* Method and the INDO/S-CI Method Compared with the Observed Solid State $\pi \rightarrow \pi^*$ Absorption Spectrum of Adenosine (Ref 28)^a

$E (\times 10^{-3} \text{ cm}^{-1})$			
CIS/6-31G*	INDO/S-CI	obsd	calcd character
36.9 ^b (0.38)	35.2 (0.12)	36.4 (0.10)	$\pi \rightarrow \pi^*$
37.4 ^b (0.04)	37.8 (0.31)	37.7 (0.20)	$\pi \rightarrow \pi^*$
41.0 ^b (0.001)	36.4 (0.005)		$n \rightarrow \pi^*$
43.5 ^b (0.004)	37.7 (0.018)		$n \rightarrow \pi^*$
45.7 ^b (0.02)	42.1 (0.021)		$n \rightarrow \pi^*$
46.2 ^b (0.33)	43.8 (0.06)	46.9 (0.25)	$\pi \rightarrow \pi^*$
	46.7 (0.008)		$n \rightarrow \pi^*$
48.6 ^b (0.46)	48.5 (0.80)	49.0 (0.33)	$\pi \rightarrow \pi^*$

^a The geometry is the MP2/6-31G* geometry as reported by Spomer and Hobza.²⁹ Numbers within parentheses are the oscillator strengths.

^b Transition energies are scaled by 0.72 to account for the difference in dynamical electron correlation in the ground state and the excited states.

tautomer in the geometrically relaxed excited state for both molecules. The lowest relaxed excited state has $\pi \rightarrow \pi^*$ character for 7H-2AMP but has $n \rightarrow \pi^*$ character for 7H-Ade. Furthermore, the amino group has been rotated 90° and is now perpendicular to the ring plane. The mechanism seems to be of the TICT type, but the charge transfer is rather small. As for the 9H tautomer, there is a semistationary point on the first excited-state potential energy surface that has $\pi \rightarrow \pi^*$ character. The predicted relative stability is calculated to be 12.5 kJ/mol for Ade and 6.1 kJ/mol for 2AMP. Thus, the 7H tautomer is much closer in energy to the 9H tautomer in the excited state than in the ground state for both molecules. If the solvent effect on the tautomeric equilibrium is of similar size as in the ground state, the two tautomers will be very close in energy in solution, giving a good chance for phototautomerism. However, the proton transfer must be fast, since the lifetime of the excited state is in the nanosecond range. Thus, the proton transfer might need a protic solvent to participate in the reaction in analogy with mechanism for proton mobility in water solution.²⁶ Santhosh and Mishra suggested that the emission spectrum of 2AMP involves two excited states: the $\pi \rightarrow \pi^*$ state of 9H-2AMP and the $n \rightarrow \pi^*$ state of 7H-2AMP.⁷ The above results support that conclusion.

Absorption and Emission Spectra. The transition energies for absorption and emission (fluorescence) are calculated with the CIS/6-31G method and the INDO/S method. In a recent work by Broo and Holmén,¹⁶ it was found that if the CIS transition energies were scaled by a constant factor of 0.72, a good agreement between the calculated and observed $\pi \rightarrow \pi^*$ transition energies of the DNA bases was obtained. The scaling is justified by the assumption that the dynamic electron correlation is of similar size in all the excited state. In Tables 1 and 2, the calculated absorption transition energies are compared with the observed absorption spectrum for Ade and 2AMP, respectively. The calculated $\pi \rightarrow \pi^*$ transition energies of Ade have already been reported in an earlier work.¹⁶ The observed absorption spectrum of both molecules is reasonably well reproduced with both methods.

The band maximum of the fluorescence spectrum corresponds to an adiabatic (vertical) transition from the geometrically relaxed excited-state to the ground-state potential energy surface at a nonequilibrium position; see Figure 3. Thus, the transition energy for the fluorescence is calculated using the geometrically relaxed excited-state geometry. The calculated fluorescence energies are collected in Table 3. It is notable that for Ade the calculated emission energy using the $\pi \rightarrow \pi^*$ excited-state

TABLE 2: 2-Aminopurine Vertical Transition Energies Predicted by the CIS/6-31G* Method and the INDO/S-CI Method Compared with the Observed Stretched Film Absorption (Ref 30)^a

$E (\times 10^{-3} \text{ cm}^{-1})$			
CIS/6-31G*	INDO/S-CI	obsd	calcd character
33.2 ^b (0.31)	33.5 (0.20)	32.8 (0.10)	$\pi \rightarrow \pi^*$
36.7 ^b (0.006)	34.2 (0.009)	~36.0	$n \rightarrow \pi^*$
38.3 ^b (0.14)	38.2 (0.34)	40.0 (0.06)	$\pi \rightarrow \pi^*$
43.9 ^b (0.015)	41.6 (0.020)		$n \rightarrow \pi^*$
46.2 ^b (0.001)	45.5 (0.000)		$n \rightarrow \pi^*$
46.7 ^b (0.049)	43.9 (0.005)	44.4 (0.19)	$\pi \rightarrow \pi^*$
47.3 ^b (0.92)	48.1 (0.63)	46.7 (0.13)	$\pi \rightarrow \pi^*$

^a The geometry is the MP2/6-31G* geometry as reported by Broo and Holmén.³¹ Numbers within parentheses are the oscillator strengths.

^b The transition energies are scaled by a factor of 0.72, to account for the difference in dynamical electron correlation in the ground state and the excited states.

TABLE 3: Calculated and Observed Fluorescence Band Maxima for Ade and 2AMP^a

	INDO/S		CIS/6-31G		obsd	
	$E (\times 10^{-3} \text{ cm}^{-1})$	f_{osc}	$E (\times 10^{-3} \text{ cm}^{-1})$	f_{osc}	$E (\times 10^{-3} \text{ cm}^{-1})$	ϕ_f
9H-A						
$n \rightarrow \pi^*$	21.7	0.01	26.8	0.01	32.2 ^b	0.5×10^{-4}
$\pi \rightarrow \pi^*$	32.0	0.11	32.4	0.46		
7H-A						
$n \rightarrow \pi^*$	23.2	0.01	27.5	0.01	32.2 ^b	8.2×10^{-4}
$\pi \rightarrow \pi^*$	28.9	0.11	31.5	0.18		
9H-2AMP						
$\pi \rightarrow \pi^*$	31.4	0.29	30.8	0.37	27.9 ^c 27.8 ^d	0.1 ^c 0.72 ^d
7H-2AMP						
$\pi \rightarrow \pi^*$	30.2	0.24	29.8	0.25		

^a The geometries used in the calculations are the CIS/6-31G optimized excited-state geometries. ^b As reported by Callis in ref 1. ^c Emission spectrum taken in ethyl ether ether.⁶ ^d Emission spectrum taken in water.³⁰

geometry (λ_3 in Figure 3) agrees much better with the observed fluorescence than when the $n \rightarrow \pi^*$ geometry is used (λ_4 in Figure 3). The avoided crossing point of the two excited states ($n \rightarrow \pi^*$ and $\pi \rightarrow \pi^*$) was located, and the electronic coupling amounts to 4200 cm⁻¹. Further, a very small barrier (0.6 kJ/mol) separates the $\pi \rightarrow \pi^*$ and the $n \rightarrow \pi^*$ state as calculated as the energy difference between the $\pi \rightarrow \pi^*$ state "equilibrium" geometry and the lowest excited state at the avoided crossing. Thus, the pseudo Jahn-Teller distortion of the excited-state potential energy surface leads to an equilibrium geometry of the first excited state that has mostly $n \rightarrow \pi^*$ character. With this small barrier and large electronic coupling the lowest singlet excited-state potential energy surface is rather flat with two (semi-) stationary points where the character of the states are a mixture of $n \rightarrow \pi^*$ and $\pi \rightarrow \pi^*$ character. Adding the zero-point vibration energy to the excited state surface will probably lead to a situation where the first vibration level is located above the barrier between the two (semi-) stationary points. Thus, the potential energy well is shallow, and the vibration levels are closely spaced. Classical motion along the surface will change both the character of the state as well as the geometry. The radiationless deactivation is caused by the large out-of-plane distortion (the six-membered ring puckering) that causes the coupling of the two first excited states. Further distortion along that out-of-plane distortion leads to an increasing overlap with the ground-state vibration states and large Franck-Condon factors for radiationless internal conversion to the ground state. Hence, an effective quenching channel for the luminescence of

Ade has been demonstrated by the calculations. It is important to note that the calculations do not include dynamical electron correlation and solvent effects. The solvent effects can be estimated from the difference in state dipole moments or be directly calculated using a self-consistent reaction field method where the solvent is represented by a dielectric continuum. Recently, Broo and Zerner developed a method to account for solvent effects on emission spectrum.²⁷ However, for both Ade and 2AMP the solvent effect on the absorption and emission spectra is rather small. The trend is that the $\pi \rightarrow \pi^*$ state is red-shifted in a polar solvent and the $n \rightarrow \pi^*$ will be blue-shifted. All the geometries reported here have been obtained in the vacuum, and no attempts have been made to include the solvent effect in the geometry calculations. Thus, it is possible that the $\pi \rightarrow \pi^*$ excited state of both tautomers of Ade will be lower in energy than the $n \rightarrow \pi^*$ state in a polar solvent. But the $n \rightarrow \pi^*$ state is 15.3 kJ/mol lower in energy in vacuum, and the state dipole moment does not indicate that a large shift is to be expected in a polar solvent. The quantum yield of 2AMP increases with increasing polarity of the solvent and decreases upon DNA binding.^{3,5,6} Obviously, the nonradiative deactivation channel is sensitive to the environment. The calculation of the tautomeric equilibrium in the excited state of 2AMP and the observed two-component decay of the emission indicates that the emission of 2AMP arises from two tautomers. However, DNA binding blocks the $7H \leftrightarrow 9H$ tautomerism. Thus, the blocked tautomerism might explain the decrease in quantum yield upon DNA binding. Further, the effect of a polar solvent is to stabilize the $\pi \rightarrow \pi^*$ state and destabilize the $n \rightarrow \pi^*$ state, leading to a larger energy separation that prevents population of the out-of-plane vibrational mode which couples the $n \rightarrow \pi^*$ state with the ground state. This nonradiative decay channel has not been demonstrated by the calculations but should be possible even if the probability will be small, especially compared to Ade.

Summary

To be able to explain the different photophysical properties of the two isomers adenine (6-aminopurine) and 2-aminopurine, the geometries of both the ground state and the lowest single excited state were calculated. Very little is known about how well different quantum chemical methods reproduce excited-state geometries of medium-sized molecules. Thus, as an initial study, the expected accuracy from calculations of the excited-state geometry was evaluated using three methods. All methods give similar excited-state geometries. The ab initio CIS method includes all possible singly substituted determinants resulting in a well-balanced description of both the ground state and the excited states. However, no dynamical electron correlation is included in the CIS wave function. The CIS method must be considered as the most reliable method and was used in the further study of excited-state tautomerism and emission spectra.

Three different possible deactivation mechanisms of the excited state were considered: the proximity effect or pseudo Jahn–Teller effect, excited-state tautomerism, and formation of twisted intramolecular charge transfer states. For both the $7H$ and $9H$ tautomer of Ade a state crossing occurred during the geometry optimization, giving an $n \rightarrow \pi^*$ character of the geometry relaxed first excited state as opposed to 2AMP where the lowest state has $\pi \rightarrow \pi^*$ character. The rather large out-of-plane distortion of the $n \rightarrow \pi^*$ state might be identified as the pseudo Jahn–Teller distortion which opens up a nonradiative deactivation channel for $7H$ -Ade and $9H$ -Ade. The physical

reason for the different behavior of the excited state of Ade and 2AMP is that the bond length alternation in the six-membered ring is dissimilar for the two molecules, giving different force constants for the out-of-plane bending mode that opens up the nonradiative deactivation channel. Further, the relative stability of the $7H$ and the $9H$ tautomers of both molecules are in less favor of the $9H$ tautomer in the excited state as compared with the ground-state relative stability. Tautomerism in the excited state might explain the difference in luminescence quantum yield upon DNA binding for 2AMP. Even more, the fully relaxed excited state of $7H$ -Ade has $n \rightarrow \pi^*$ character with the amino group rotated 90° with respect to the ring plane. The charge transfer from the ring system to the amino group is rather small, but the mechanism is similar to what is observed in so-called TICT states. The calculations suggest that the emission for both tautomers of Ade probably starts from a point on the excited-state surface that mostly has $\pi \rightarrow \pi^*$ character, however, with very small quantum yield since the nonradiative decay is so effective.

Acknowledgment. This work was financed by grants from the Swedish Science Research Council (NFR). The National Supercomputer Center (NSC) at Linköping, Sweden, and the Center for parallel computers (PDC) at Stockholm, Sweden, are acknowledged for generous supply of computer time.

References and Notes

- (1) Callis, P. R. *Annu. Rev. Chem.* **1983**, *34*, 329.
- (2) Fletcher, A. N. *J. Mol. Spectrosc.* **1967**, *23*, 221.
- (3) Ward, D. C.; Reich, E.; Stryer, L. *J. Biol. Chem.* **1969**, *244*, 1228.
- (4) Nordlund, T. M.; Andersson, S.; Nilsson, L.; Rigler, R.; Gräslund, A.; McLaughlin, L. W. *Biochemistry* **1989**, *28*, 9095. Guest, C. R.; Hochstrasser, R. A.; Sowers, L. C.; Millar, D. P. *Biochemistry* **1991**, *30*, 3271. Bloom, L. B.; Otto, M. R.; Beechem, J. M.; Goodman, M. F. *Biochemistry* **1993**, *32*, 11247. Hochstrasser, R. A.; Carver, T. E.; Sowers, L. C.; Millar, D. P. *Biochemistry* **1994**, *33*, 11971.
- (5) Fletcher, A. N. *J. Mol. Spectrosc.* **1967**, *23*, 211.
- (6) Smagowicz, J.; Wierchowski, K. L. *J. Lumin.* **1974**, *8*, 210.
- (7) Santhosh C.; Mishra, P. C. *Spectrochim. Acta* **1991**, *47A*, 1685.
- (8) Longworth, J. W.; Rahn, R. O.; Shulman, R. G. *J. Chem. Phys.* **1966**, *45*, 2930.
- (9) Eastman, J. W. *Ber. Bunsen-Ges. Phys. Chem.* **1969**, *75*, 407.
- (10) Wilson, R. W.; Callis, P. R. *Photochem. Photobiol.* **1980**, *31*, 323.
- (11) Lim, E. C. *J. Phys. Chem.* **1986**, *90*, 6770.
- (12) Hochstrasser, R. M.; Marzocco, C. A. In *Molecular Luminescence*; Lim, E. C., Ed.; Benjamin: New York, 1969; p 631.
- (13) Albinsson, B. *J. Am. Chem. Soc.* **1997**, *119*, 6369.
- (14) AM1: Dewar, M. J. S.; Zoebish, E. G.; Healy, E. F.; Stewart, J. J. P. *J. Am. Chem. Soc.* **1985**, *107*, 3902.
- (15) Mopac 6.0, Program 455, Quantum Chemistry Program Exchange.
- (16) Broo, A.; Holmén, A. *J. Chem. Phys.* **1997**, *101*, 3589.
- (17) Gaussian 94: Frisch, M. J.; Trucks, G. W.; Schlegel, H. B.; Gill, P. M. W.; Johnson, B. G.; Robb, M. A.; Cheeseman, J. R.; Keith, T.; Petersson, G. A.; Montgomery, J. A.; Raghavachari, K.; Al-Laham, M. A.; Zakrzewski, V. G.; Ortiz, J. V.; Foresman, J. B.; Peng, C. Y.; Ayala, P. Y.; Chen, W.; Wong, M. W.; Andres, J. L.; Replogle, E. S.; Gomperts, R.; Martin, R. L.; Fox, D. J.; Binkley, J. S.; Defrees, D. J.; Baker, J.; Stewart, J. P.; Head-Gordon, M.; Gonzalez, C.; Pople, J. A. Gaussian, Inc., Pittsburgh, PA, 1995.
- (18) GAMESS: Schmidt, M. W.; Baldridge, K. K.; Boatz, J. A.; Elbert, T. S.; Gordon, M. S.; Jensen, J. H.; Koseki, S.; Matsunaga, N.; Nguyen, K. A.; Su, S.; Windus, T. L.; Dupuis, M.; Montgomery Jr., J. A. *J. Comput. Chem.* **1993**, *14*, 1347.
- (19) The 6-31G basis set: Hariharan, P. C.; Pople, J. A. *Theor. Chim. Acta* **1973**, *28*, 21.
- (20) ZINDO: Zerner, M. C. Quantum Theory Project, University of Florida, Gainesville, FL 32611. Ridley, J. E.; Zerner, M. C. *Theor. Chim. Acta* **1973**, *32*, 111; **1976**, *42*, 223.
- (21) Lezczynski, J. *Int. J. Quantum Chem.* **1992**, *QBS19*, 43.
- (22) Stewart, E. L.; Foley, G. K.; Allinger, N. L.; Bowen, J. P. *J. Am. Chem. Soc.* **1994**, *116*, 7282.

- (23) Sponer, J.; Hobza, P. *J. Phys. Chem.* **1994**, 98, 3161.
(24) Holmén, A.; Broo, A. *Int. J. Quantum Chem.* **1995**, QBS22, 113.
Broo, A.; Holmén, A. *Chem. Phys.* **1996**, 211, 147.
(25) Broo, A. Manuscript under preparation.
(26) See for instance: Alberty, R. A. In *Physical Chemistry*, 5th ed.; John Wiley & Sons: New York; p 585.
(27) Broo, A.; Zerner, M. C. *Theor. Chim. Acta* **1995**, 90, 383. Broo, A.; Zerner, M. C. *Chem. Phys. Lett.* **1994**, 227, 551.
(28) Clark, L. B. *J. Phys. Chem.* **1995**, 99, 3366.
(29) Sponer, J.; Hobza, P. *J. Phys. Chem.* **1994**, 98, 3161.
(30) Holmén, A.; Nordén, B.; Albinsson, B. *J. Am. Chem. Soc.*, in press.
(31) Broo, A.; Holmén, A. *Chem. Phys.* **1996**, 211, 147.